

Article

Microstructure and Properties of Polytetrafluoroethylene Composites Modified by Carbon Materials and Aramid Fibers

Fubao Zhang *, Jiaqiao Zhang , Yu Zhu, Xingxing Wang and Yuyang Jin

School of Mechanical Engineering, Nantong University, Nantong 226019, China; 1810310038@stmail.ntu.edu.cn (J.Z.); zhuyu.ntu@gmail.com (Y.Z.); wangxx@ntu.edu.cn (X.W.); jinyuyang.ntu@gmail.com (Y.J.)

* Correspondence: zhang.fb@ntu.edu.cn; Tel.: +86-13646288919

Received: 12 October 2020; Accepted: 16 November 2020; Published: 18 November 2020



Abstract: Polytetrafluoroethylene (PTFE) is polymerized by tetrafluoroethylene, which has high corrosion resistance, self-lubrication and high temperature resistance. However, due to the large expansion coefficient, high temperature will gradually weaken the intermolecular bonding force of PTFE, which will lead to the enhancement of permeation absorption and the limitation of the application range of fluoroplastics. In order to improve the performance of PTFE, the modified polytetrafluoroethylene, filled by carbon materials and aramid fiber with different scales, is prepared through the compression and sintering. Moreover, the mechanical properties and wear resistance of the prepared composite materials are tested. In addition, the influence of different types of filler materials and contents on the properties of PTFE is studied. According to the experiment results, the addition of carbon fibers with different scales reduces the tensile and impact properties of the composite materials, but the elastic modulus and wear resistance are significantly improved. Among them, the wear rate of 7 μm carbon fiber modified PTFE has decreased by 70%, and the elastic modulus has increased by 70%. The addition of aramid fiber filler significantly reduces the tensile and impact properties of the composite, but its elastic modulus and wear resistance are significantly improved. Among them, the wear rate of the modified composite material with 3% alumina particles and 5% aramid pulp decreased by 68%, and the elastic modulus increased by 206%.

Keywords: polytetrafluoroethylene; carbon material; aramid fiber; material modification

1. Introduction

PTFE is polymerized by tetrafluoroethylene, and its molecular chain is $-\text{CF}_2-\text{CF}_2-\text{}$ ^{*n*}. In detail, the conformation of PTFE molecular chain presents a spiral structure, and the C–F bond is one of the strongest chemical bonds, making the main chain structure of PTFE very stable [1]. PTFE has incomparable corrosion resistance, self-lubrication and high and low temperature resistance, which are unmatched by metal materials [2]. Thus, it is often used on the surface of some objects, such as textiles [3,4], valves [5], pipes [6], etc., through the fluorine lining process. Especially when PTFE is used as a sealing material, it is necessary to increase the elastic modulus of PEFT to prevent creep phenomenon [7], which will lead to leakage. Therefore, how to improve the corrosion resistance and elastic modulus of PTFE and expand the application range of PTFE on the surface of engineering objects has become a research hotspot [8].

The filling is one of the simplest and most effective modification methods for fluoroplastics [9,10]. More specifically, by adding fillers to the fluoroplastic matrix, the crystal structure of the fluoroplastic is changed, thereby improving and overcoming the original defects of the fluoroplastic [11]. The materials

filled with modified PTFE mainly include carbon materials and aramid fibers [12,13]. In the modification of PTFE-filled fiber, the fiber mainly plays the role of bearing, and the matrix material plays the role of bonding the fibers firmly to each other and transferring the load to the fibers. Carbon fiber (CF) is a new type of fiber material with the carbon content of more than 95% after carbonization and graphitization of organic fibers [14,15]. The CF has excellent corrosion resistance and high temperature resistance, which is widely used as a high-quality filler or performance improver for rubber, plastic and various composite materials. Multiwalled carbon nanotube (MWCNT) is a quantum material with a special structure, which has good mechanical properties and more stable structure than polymers [16]. It is commonly used as the enhancer to improve the strength, elasticity and fatigue resistance of composite materials. Kevlar poly-p-phenylene terephthamide (PPTA) is a synthetic fiber with ultra-high strength and abrasion resistance [17]. PPTA has a high elastic modulus and excellent dimensional stability, and is widely used in the filling modification of polymer materials [18]. Al_2O_3 is a kind of metal aluminum oxide [19–21], it is often used as an inorganic filler to improve the hardness and wear resistance of modified PTFE materials. Due to the lack of necessary affinity between the inorganic filler and the PTFE interface, the combination of the two is poor, resulting in a decrease in the tensile strength, elongation, impact performance and compression rate of the modified PTFE material.

Scholars have conducted many studies on modification experiments of PTFE, and certain properties of PTFE have been improved. A.P. Vasilev studied the effect of composite fillers on the properties and structure of PTFE, and confirmed that the introduction of composite fillers significantly improved the wear resistance of PTFE composites [22]. A.A. Ohlopkova studied the effect of carbon fiber on the performance and structure of polytetrafluoroethylene. It is proved that carbon fiber can improve the tribological properties of PTFE [23]. Prateek Saxena et al. used a variety of filler materials to improve the frictional mechanical properties of cyanate ester, and proved that graphite produced the best effect among all fillers used, offering a lower specific wear rate, a lower friction value and a higher tensile strength and tensile modulus [24]. In addition, Prateek Saxena's team has developed a new type of testing device to identify the friction characteristics of carbon fiber reinforced polymer composites under high surface pressure, which is conducive to the performance testing of polymer materials [25]. Fuchuan Luo et al. used $\text{Na}_{1/2}\text{Sm}_{1/2}\text{TiO}_3$ and glass fiber to fill PTFE to improve the electrical conductivity of PTFE composites [26]. YingYuan et al. prepared a kind of PTFE composite material filled with Si_3N_4 . As the content of Si_3N_4 increases, the electrical conductivity and thermal conductivity of the PTFE composite material are improved [27]. L.J. van Rooyen et al. used graphene oxyfluoride to fill PTFE, thereby reducing the permeability of PTFE. The incorporation of the oxyfluorinated and commercial grade graphene into the PTFE reduced the helium gas permeability by 96% at 4 vol.% and by 88% at 7 vol.% nanofiller contents, respectively [28].

Compared with previous studies, this article innovatively uses carbon nanotubes and aramid fibers to fill modified PTFE, thereby improving the wear resistance and elastic modulus of the composite material, making it more suitable for engineering object surfaces and seals. Starting from the modification process of fluoroplastics, this paper studies the influence of different types of filler materials on the properties of PTFE, and analyzes the mechanism of the influence of filler content on the properties of PTFE. Our research has effectively improved the wear resistance and elastic modulus of PTFE materials, which is conducive to the use of PTFE on the surface and seals of engineering objects, and provides scientific basis and reference for the research and practical application of new PTFE composite materials.

2. Materials and Instruments

2.1. Experimental Materials

The main reagents and materials used in the experiment are shown in Table 1.

Table 1. Main reagents and materials used in the test.

Reagent Name	Reagent/Material Manufacturer	Description of Product Codes
PTFE	Japan Daikin Fluorochemical (China) Co., Ltd. (Changshu, China)	Particle size of 20 μm
7 μm carbon fiber	Chuangjia Welding Material Co., Ltd. (Qinghe, China)	Length of 50 μm , monofilament diameter of 7 μm
200 nm carbon fiber	Shanghai Alighting Biochemical Technology Co., Ltd. (Shanghai, China)	Length of 5–50 μm , outer diameter of 200–600 nm
Multi-walled carbon nanotubes	Shanghai McLean Biochemical Technology Co., Ltd. (Shanghai, China)	Carboxylation, length of 50 μm , inner diameter of 3–5 nm, outer diameter of 8–15 nm, –COOH content of 2.6 wt.%
Aramid Pulp	Dupont China Group Co., Ltd. (Shenzhen, China)	Kevlar 1F1710, length of 0.7–1.6 mm
Al_2O_3	Mingshan New Materials Co., Ltd. (Laiwu, China)	Powder, particle size of 30–40 nm
Titanate coupling agent	Ding Hai Plastic Chemical Co., Ltd. (Dongguan, China)	KH-792
Absolute ethanol	Sinopharm Chemical Reagent Co., Ltd. (Shanghai, China)	Analytical reagent
Acetic anhydride	Jiangsu Qiangsheng Functional Chemical Co., Ltd. (Changshu, China)	Analytical reagent
Acetone	Shanghai Lingfeng Chemical Reagent Co., Ltd. (Shanghai, China)	Analytical reagent

2.2. Experimental Instruments

The main performance test instruments used to complete all the tests are shown in Table 2.

Table 2. Main test and analysis instruments used in the experiment.

Device Name	Device Model	Vendor
Compressive and flexural testing machine	YAW-300C	Jinan Dongfang Experimental Instrument Co., Ltd. (Jinan, China)
Shore Hardness Tester	LX-D type	Nanjing Suce Measuring Instruments Co., Ltd. (Nanjing, China)
Scanning electron microscope	S-3400N	Hitachi Manufacturing Co., Ltd. (Tokyo, Japan)
Transmission electron microscope	JEM-2100hr	Japan Electronics Corporation (Tokyo, Japan)
Pendulum impact sample machine	E45.105	MTS Industrial Systems Co., Ltd. (Shenzhen, China)
Universal testing machine	CMT5105	MTS Industrial Systems (China) Co., Ltd. (Shenzhen, China)
Friction and wear tester	MFT-V	American Rtec Equipment Co., Ltd. (San Jose, CA, USA)

2.3. Performance Testing and Organization Analysis Methods

The hardness testing shall be conducted in accordance with GB/T2411-2008 [29] Plastics and Ebonite Determination of Indentation Hardness (Shore hardness) using a Durometer. The LX-D plastic shore hardness tester was used to measure the shore hardness of friction and wear samples, using a D type indenter with a total test force of 588.4 N. Each sample measured 5 points, and the results are represented by the arithmetic mean of the 5 measured values.

The tensile testing was carried out in accordance with GB/T1040-2006 [30] Determination of Tensile Properties of Plastics. According to the standard, the sample was processed into a rectangular spline of 80 mm \times 10 mm \times 4 mm, and then tested on the electronic tensile testing machine of CMT5504 model at a beam speed of 10 mm/min. Three samples were prepared for each test, and the final results were

taken as the tensile strength, elastic modulus and elongation at break according to the average value of the three samples.

The impact testing shall be conducted in accordance with GB/T1043-2008 [31] Determination of Impact Performance of Plastic Simply Supported Beams. According to the standard, the sample was processed into 80 mm × 10 mm × 4 mm with a depth of 2 mm A-shaped notch, and then the notched sample impact strength was measured on the combined impact tester of ZBC3000 model. The maximum impact energy of the pendulum was 7.5 J. Three samples were prepared for each test, and the final result is the average value of the three samples to express its impact toughness.

The friction and wear test was performed on the friction and wear tester of MFT-V model. The complex friction test method was adopted. The specific steps were to fix the sample on the chassis and reciprocate with the chassis. The grinding parts were made of cylindrical Cr15 bearing steel with a diameter of 5 mm, the friction stroke was set to 20 mm, the acceleration time was set to 1 s, and the reciprocating frequency was set to 2 Hz. The experiment was carried out under the load of 98 N, and the wear time was 30 min.

Impact section and wear surface morphology were performed by the following steps: first, the cross-section of the impact sample and the surface wave of the friction and wear sample were sprayed with gold to increase the conductivity of the composite material. Then, S-3400N scanning electron microscope (SEM) was used to observe the impact section and wear surface morphology under high magnification.

3. Preparation of Samples

3.1. Preparation of Carbon Material Modified PTFE

3.1.1. Surface Treatment of Carbon Fiber

Carbon fiber and nano Al₂O₃ ceramic particles are inorganic particles, which have poor binding properties with PTFE. Therefore, it is necessary to modify the surface of carbon fiber by the titanate coupling agent [32,33]. More specifically, the titanate coupling agent is coupled by its alkoxy group directly with the trace carboxyl groups or hydroxyl groups adsorbed on the surface of the filler or pigment to couple, thereby effectively improving the bonding strength between carbon fiber and PTFE.

3.1.2. Preparation of Modified PTFE

First of all, the filling modification needs to solve the problem of the dispersibility of the filler in PTFE, because the dispersion of the filler in the PTFE matrix will directly affect the performance of the composite material.

In this paper, the dry-wet mixing method was used to mix the composite materials [34], and the SEM micrograph of the carbon fiber used is as shown in Figure 1. First, the pretreated PTFE powder and carbon materials were weighed according to the mass percentage. Then, a certain amount of ethanol solution was poured into it and ultrasonic dispersion was performed for 30 min. In the next step, the PTFE powder after being stirred by a high-speed mixer and sieved was slowly poured into the stirring ethanol solution. It should be noted that the solution was stirred at high speed under the condition of heating in a water bath until the mixture shows a jelly without stratification. It is necessary to prevent the delamination of the solution during mixing. Then, the solution was placed in a drying cabinet at 80 °C for drying. The dried mixture was crushed by a high-speed crusher for 5 min and then sieved with a 100-mesh sieve to further ensure the homogeneity of the mixture. Then, the powder was placed in a mold for cold pressing to obtain a preformed sample. Next, the preformed sample was sintered in a box-type electric furnace to obtain a composite sintered sample. Finally, the test sample was cut with a punching knife for testing. The modified PTFE test sample is shown in Figure 2.

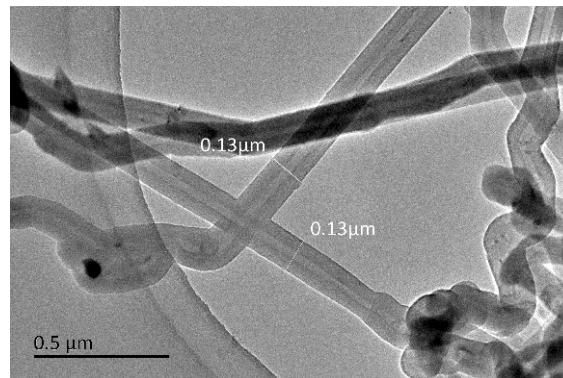


Figure 1. The SEM micrograph of the carbon fiber.

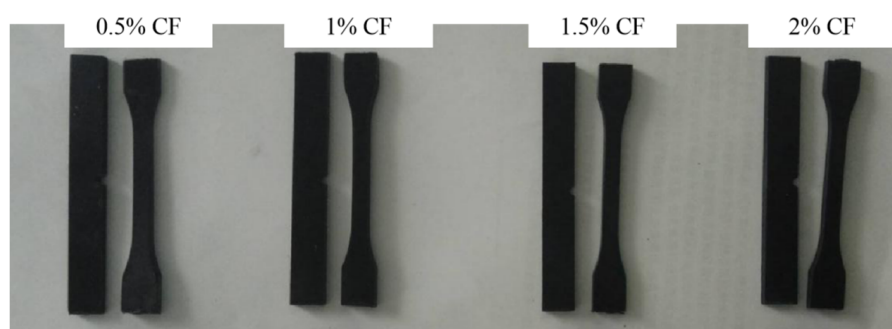


Figure 2. Test sample of carbon fiber (CF) modified PTFE composite.

3.2. Preparation of the Aramid Modified PTFE Material

3.2.1. Surface Treatment of the Aramid Fiber

The surface of the product often produces some defects during processing [35]. In order to ensure the cleanliness of the PPTA surface, it is necessary to clean the PPTA first. The detailed cleaning method is to soak PPTA in acetone for 1 h, then boil it with absolute ethanol and distilled water, and then filter the mixture and put it in an oven to dry for later use. The wastewater is treated in a harmless manner [36,37]. The SEM morphology of the PPTA surface is shown in Figure 3a. It can be seen that there are more attachments on the surface of PPTA. The SEM morphology of PPTA after cleaning with acetone is shown in Figure 3b. It can be seen that the surface of PPTA fiber was smoother after cleaning, and there was no obvious adhesion remaining. Therefore, the latter was more conducive to increasing the bonding force between the fiber and the resin matrix.

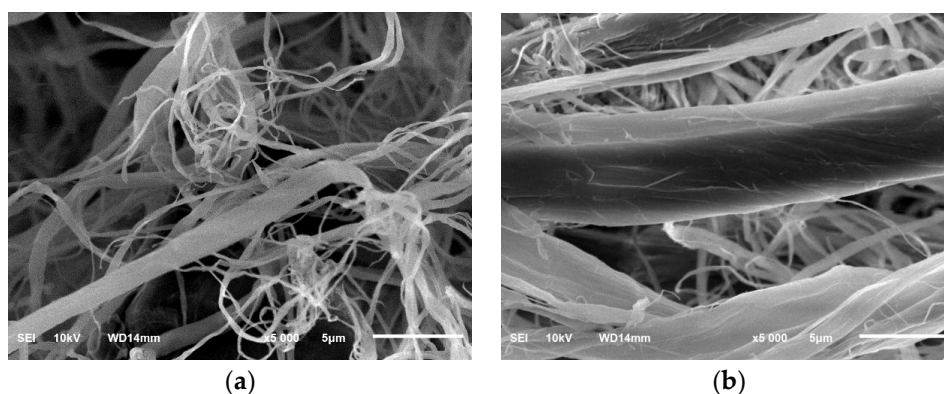


Figure 3. SEM micrographs of aramid fiber: (a) untreated aramid fiber and (b) aramid fiber after cleaning with acetone.

In order to further improve the bonding performance of PPTA and PTFE, acetic anhydride was used to modify the surface of PPTA to increase the contact area between PPTA and PTFE matrix [38]. The treatment process was that pour the acetic anhydride solution with a purity specification of analytical reagent into a beaker, and then the PPTA was immersed in the solution. Place the beaker in a water bath and heat to 70 °C and keep it for 1 h. Then, the PPTA was cleaned with ultrapure water and dried for use. The SEM morphology of PPTA fiber surface after acetic anhydride surface treatment is shown in Figure 4.

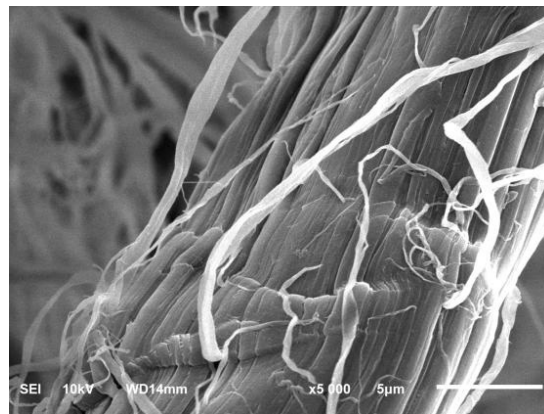


Figure 4. SEM image of aramid fiber after surface treatment with acetic anhydride for 1 h.

It can be seen from Figure 4 that there were obvious etching marks on the surface of PPTA after modification with acetic anhydride. The surface roughness and the specific surface area of PPTA after etching increased. Therefore, during the molding process of the composite material, PTFE was filled into the cavities on the surface of PPTA fiber, which caused uneven and interlaced interfaces between the fiber and the matrix material after cooling. This not only effectively increased the mechanical chimerism with the PTFE matrix, but also improved the bonding strength between the interfaces.

3.2.2. Preparation of Aramid Fiber and Nano Al₂O₃ Modified PTFE Material

The blending method adopts the mixing method combining dry and wet methods. The detailed steps are as follows. First of all, the pretreated powder and reinforcer were weighed according to the mass percentage, and a certain amount of ethanol solution was poured into a high-speed mixer for mixing. Then, the sieved PTFE powder was slowly poured into the stirring ethanol solution, and then placed in a drying oven at 80 °C for drying and cold-pressed into preformed samples. The preformed sample was put into a box-type electric furnace for sintering to form a composite material sample. Finally, the sample was cut into test specimens with a punching knife for testing. Test samples of composite materials are shown in Figure 5.

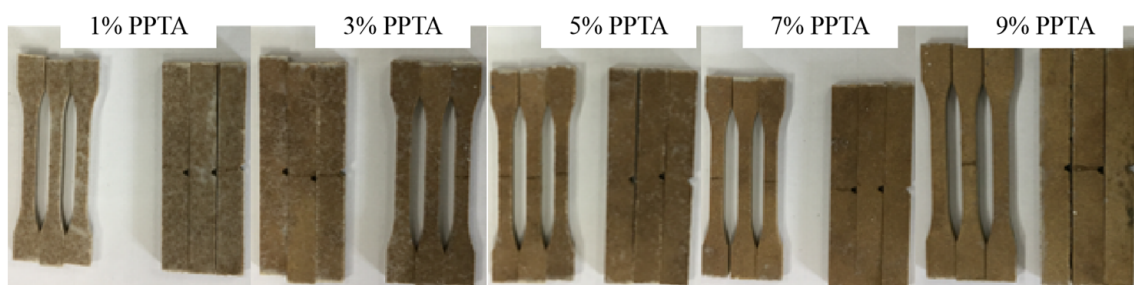


Figure 5. Test sample of PPTA and nano Al₂O₃ filled modified PTFE composite material.

4. Experimental Results and Discussion

4.1. The Structure and Properties of Carbon Material Modified PTFE Composite

4.1.1. Hardness

The impact of different types and contents of carbon materials on the hardness of filled with modified PTFE is shown in Figure 6. During the experiment, we tested each set of the data five times, and calculated the average and standard deviation. It can be seen from Figure 5 that the hardness of PTFE decreased slightly after adding different carbon materials. Among them, the hardness of PTFE composites filled with MWCNT decreased most significantly. When the filling amount of MWCNT was 1%, the hardness of the composite material decreased from 62 to 52, which was 15.3%. With the increase of the content of MWCNT, the hardness rebounds. When the filling amount of 200 nm CF was 1%, the hardness of the composite material dropped from 62 to 58.2, with a decrease of 4.8%. When the filling amount of 7 μm CF was 0.5%, the hardness of the composite material dropped from 62 to 59.6, with a decrease of 5.9%.

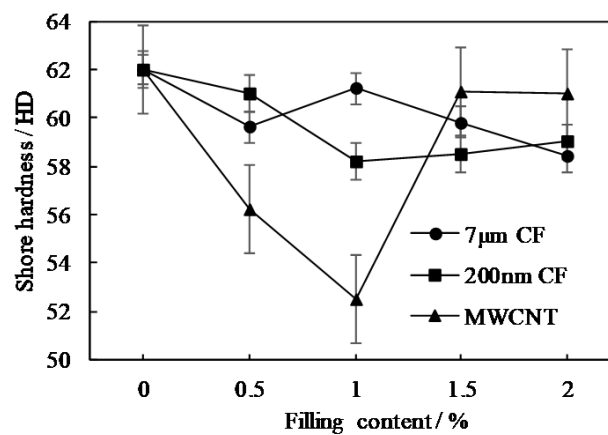


Figure 6. Hardness of micro/nano CF and multiwalled carbon nanotube (MWCNT) filled modified PTFE composites.

4.1.2. Impact Performance

The impact toughness of PTFE composites filled with micro/nano CF and MWCNT was tested. The impact performance of PTFE modified by different carbon materials is shown in Figure 7. It can be seen from the figure that the addition of CF and MWCNT reduced the impact strength of the composite material. Among them, when the filling amount of MWCNT was 1%, the impact toughness of the composite material decreased from 17.89 to 8.73 kJ/m^2 , with a decrease rate of 51%. Subsequently, with the increase of the filling amount, the impact toughness tended to stabilize. When the 200 nm CF filling amount was 0.5%, the impact toughness of the composite material decreased from 17.89 to 9.5 kJ/m^2 , with a decrease rate of 47%. Subsequently, as the filling amount increased, the impact toughness tended to stabilize. When the filling amount of 7 μm CF was 1%, the impact toughness of the composite material decreased from 17.89 to 8.61 kJ/m^2 , with a decrease rate of 55%. Subsequently, as the filling amount increased, the impact toughness slowly rose. The reason is that the mechanical chimerism between the matrix material and the modified material lacked sufficient flexibility, which is prone to brittle fracture when bearing an impact. In addition, the bonding strength between CF and MWCNT and the matrix material was poor, and the energy of an impact fracture cannot be effectively transferred between the composite materials.

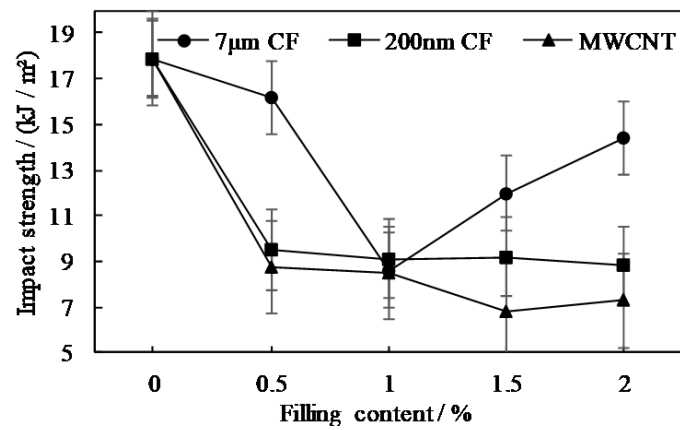


Figure 7. Impact properties of micro/nano CF and MWCNT modified PTFE.

4.1.3. Tensile Performance

The tensile strength, tensile elongation at break and elastic modulus of CF and MWCNT modified PTFE composites with different contents are shown in Figures 8–10.

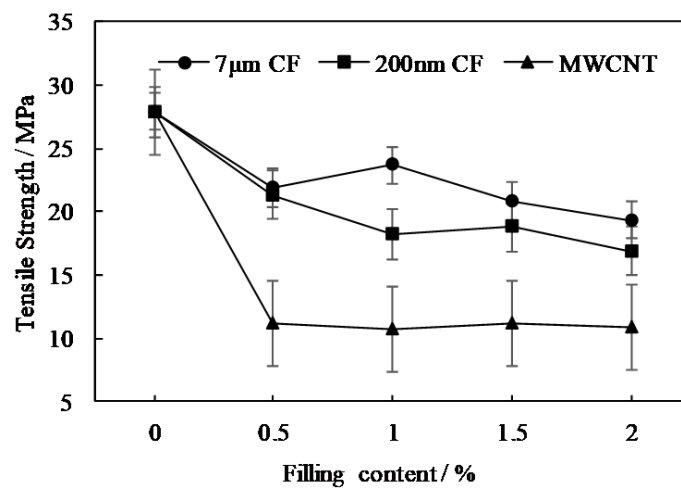


Figure 8. Tensile strength of micro/nano CF and MWCNT modified PTFE composites.

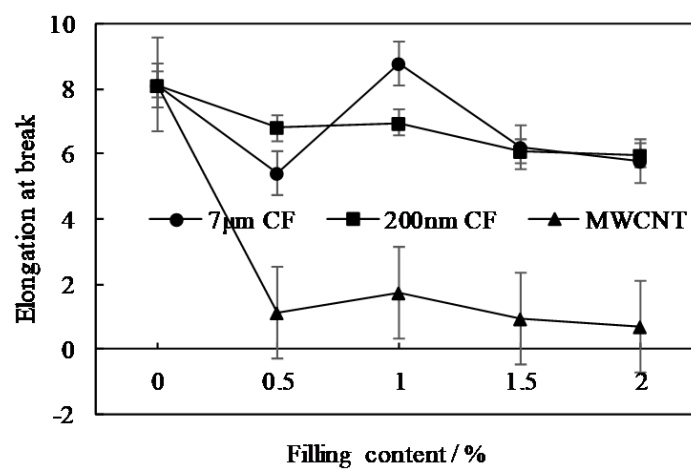


Figure 9. Tensile elongation at break of micro/nano CF and MWCNT modified PTFE composites.

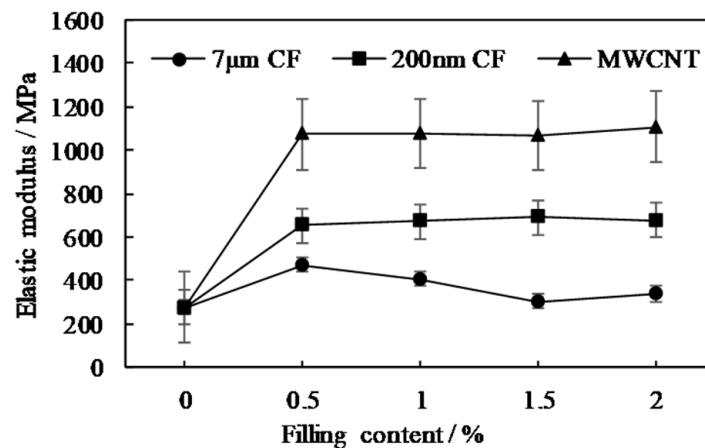


Figure 10. Elastic modulus of micro/nano CF and MWCNT modified PTFE composites.

It can be seen from Figures 8 and 9 that the tensile strength and elongation at break of PTFE were significantly reduced after adding CF and MWCNT. Among them, when the addition amount of 7 µm CF was 0.5%, the tensile strength of the PTFE composite material decreased from 27.9 to 21.87 MPa, which was about 20%, and the tensile elongation at break decreased from 810% to 541%. With the increase of CF to 1%, the tensile strength of the composite material increased to 23.64 MPa, and the tensile elongation at break also rose to the original level. Then, as the CF increased, the tensile strength slowly decreased. Compared with CF, when the addition amount of MWCNT was 0.5%, the tensile strength and tensile elongation at break of PTFE composites dropped significantly to 11.19 MPa and 111%, respectively, with a decrease of about 60% and 87%.

It can be seen from Figure 10 that the elastic modulus of the composite can be effectively improved by adding CF and MWCNT. Among them, the addition of 7 µm and 200 nm CF increased the elastic modulus of PTFE by about 70% to 471.95 MPa and 137% to 655 MPa from the original 276.8 MPa. Then, as the filler increased, the elastic modulus of the composite material tended to stabilize. In contrast, MWCNT had a greater impact on the elastic modulus of PTFE composites. The addition of 1% MWCNT increased the elastic modulus of PTFE from 276.8 to 1075 MPa, with the increase of about 388%. Then, as the filler content increased, the change in the elastic modulus was smaller.

By comparing the tensile properties of 200 nm CF filled composites and 7 µm CF filled composites, it can be seen that the elastic modulus of the former had doubled that of the latter, but there was no significant difference between the tensile properties and the tensile fracture productivity. Therefore, it could be concluded that nano-level CF could effectively improve the stiffness of PTFE. When the addition amount of nano CF reached 1.5%, the elastic modulus of the composite material began to decrease, indicating that the excessive CF had a negative effect on the elastic modulus of PTFE. The reason is that with the increase of CF content, CF agglomerates become an impurity point of the composite, which can not further improve its mechanical properties. Compared with the composite filled with CF and MWCNT, it can be seen that MWCNT can significantly enhance the elastic modulus of the composite, but its tensile properties and tensile elongation at break were significantly reduced. This may be because compared with CF, MWCNT had a smaller diameter and more uniform dispersion and larger contact area in PTFE matrix materials. These conditions make it easier to restrict the slippage of PTFE macromolecules, which can effectively increase the elastic modulus of the composite material. However, because the C–C bond in PTFE is wrapped by F atoms, and the F atoms are relatively stable, CF and MWCNT cannot generate a strong chemical bond link with the PTFE matrix, but only through simple physical bonding. During the stretching process, the stress on the PTFE matrix material cannot be transferred to the filler material, which leads to the decrease of the tensile strength of the composite.

In order to further study the influence of different carbon materials and different scale carbon materials on the properties of PTFE composites and the strengthening mechanism, the tensile section

of the sample was observed by a scanning electron microscope. In this study, gold was sprayed on the section of the tensile specimen and the surface of the friction and wear specimen, and then the impact section and the wear morphology surface were observed under high magnification using SEM. The SEM of the tensile fracture surface is shown in Figure 11.

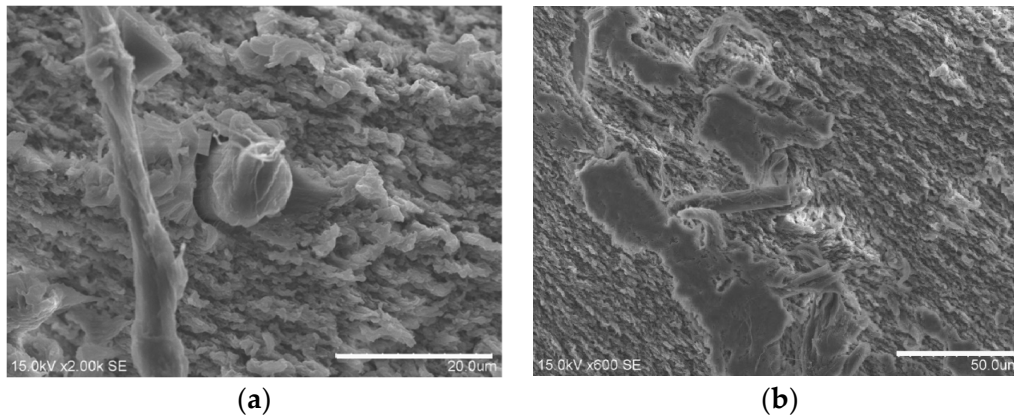


Figure 11. SEM image of the 1% 7 μm CF-filled PTFE tensile section: (a) the magnification 2000 \times ; (b) the magnification 600 \times .

It can be seen from Figure 11 that there was CF perpendicular/parallel to the tensile fracture plane. Furthermore, there were certain gaps between the CF and the matrix. These voids easily caused stress concentration, which induced and propagated cracks. Then, the cracks propagated along with the interface, causing the interface to be damaged, and the CF was pulled out of the matrix material, and finally the tensile properties of the composite material were reduced. The fracture mode of the composite material was the fiber/matrix debonding fiber pull-out. Under the action of external force, the interface bonding performance determines the stress transfer effect between the fiber and the matrix, which in turn affected the failure mechanism of the composite material, and ultimately affected the macroscopic mechanical properties of the composite material.

4.1.4. Friction and Wear Performance

The study tested the friction and wear of micro/nano CF and MWCNT filled modified PTFE composites. The friction coefficient and wear rate of the composite material are shown in Figures 12 and 13.

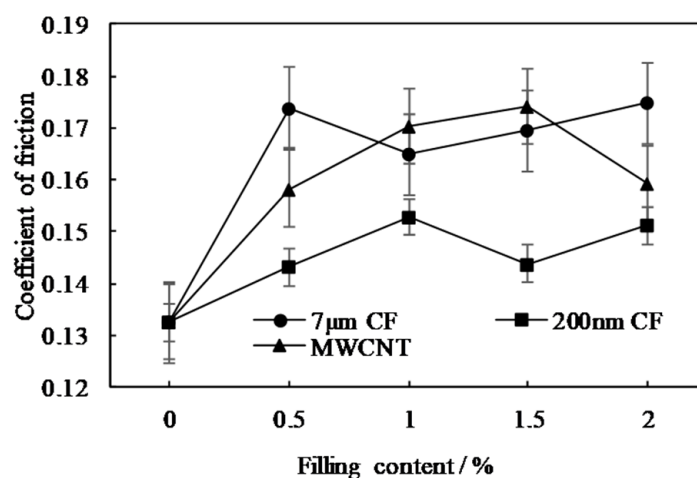


Figure 12. Friction coefficient of micro/nano CF and MWCNT filled modified PTFE composites.

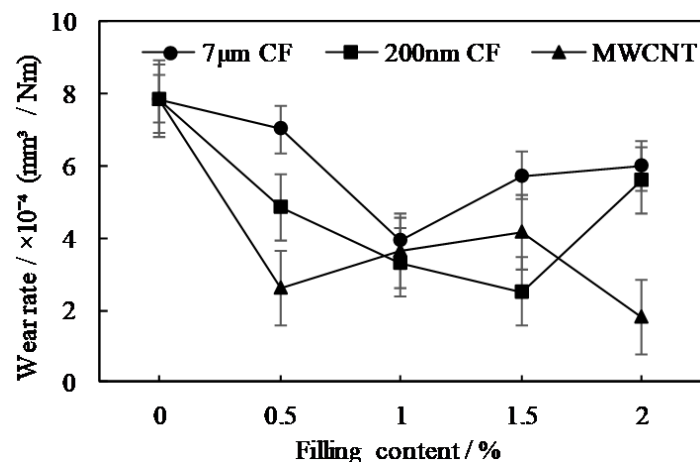


Figure 13. Wear rate of micro/nano CF and MWCNT filled modified PTFE composites.

It can be seen from Figure 12 that the addition of different carbon materials slightly increased the friction coefficient of the composite material. It can be seen from Figure 13 that the strength and load-bearing capacity of the composite material were improved, indicating that the ability of the composite material to resist plastic deformation was significantly improved, and the ploughing effect of the grinding parts on the surface of the composite material was reduced. The addition of CF and MWCNT has greatly improved the wear resistance of composite materials. Under the experimental conditions, as the content of different types of carbon materials increased, the wear of composite materials decreased significantly. Among them, when 7 µm CF was used as the modified filler and the mass fraction was 1.5%, the wear rate of the composite material dropped from 7.8463×10^{-4} to 2.5124×10^{-4} mm³/Nm, a decrease of 58%. Subsequently, the wear rate of the composite material increased slightly. When 200 nm CF was used as a modified filler and the mass fraction was 1%, the wear rate of the composite material decreased from 7.8463×10^{-4} to 3.9038×10^{-4} mm³/Nm, a decrease of 50.3%. Then the wear rate gradually increased. When MWCNT was used as a modified filling and the mass fraction was only 0.5%, the wear rate of the composite material decreased from 7.8463×10^{-4} to 2.5897×10^{-4} mm³/Nm, a decrease of 57%. Subsequently, the wear rate increased slowly, but the wear rate remained below 50% of the unmodified PTFE.

In order to further study the mechanism of filler material on the wear performance of composite materials, the wear surface was tested by scanning electron microscopy. The surface morphology of different carbon materials after wear is observed, as shown in Figure 14.

According to Figure 14, there was no obvious crack on the surface of the composite material. However, there was adhesive wear of the PTFE matrix. In addition, no obvious dents left by carbon CF exposure or peeling of carbon fiber were seen on the PTFE surface. Due to its good self-lubricity, PTFE is easy to form a thin crystalline layer. The crystalline layer and the amorphous layer were alternately arranged in a strip structure. In addition, because of the low friction coefficient, the amorphous partial layer was easy to slide. Since PTFE has a strong intramolecular structure and weak intermolecular binding force, macromolecules are prone to slippage under external force. The essence of PTFE wear is that the macromolecules slip and break under the action of external force, so that the material is pulled out of the crystallization zone and transferred to the surface of the mating part in a sheet shape, resulting in adhesive wear. The addition of CF in PTFE can improve its compressive strength. When the composite is in the process of reciprocating friction and wear, CF mainly plays the role in bearing and limiting the PTFE macromolecular sliding, so it effectively improves the wear resistance of the composite.

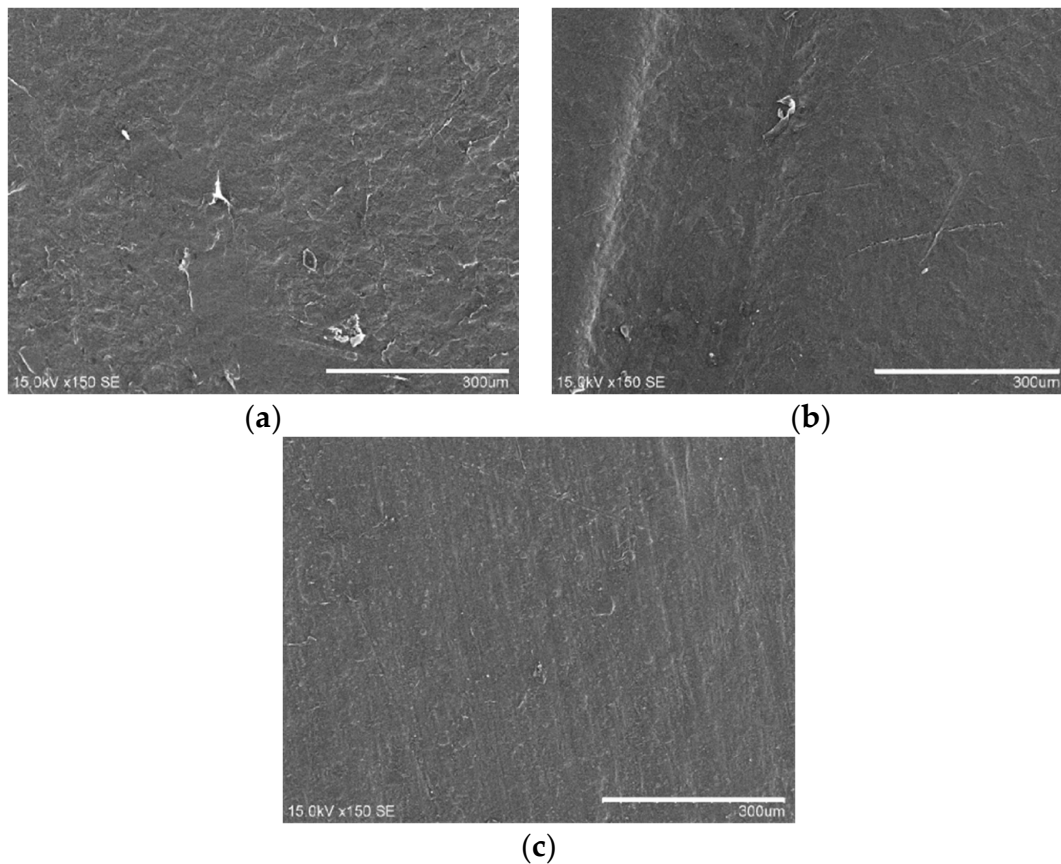


Figure 14. SEM diagram of PTFE wear surfaces filled with different carbon materials: (a) 1% 7 μm CF; (b) 1% 200 nm CF and (c) 1% MWCNT.

4.2. Structure and Properties of the Aramid Modified PTFE Composite

4.2.1. Hardness

The hardness test of PPTA and nano Al_2O_3 filled modified PTFE was conducted. The hardness of the composite material is shown in Figure 15. It can be seen from the figure that after PPTA was added, the hardness of PTFE decreased slightly. When the amount of PPTA added was 1%, the shore hardness of the composite material dropped from 62 to 59.2, a decrease of 4.5%. Subsequently, the hardness of the composite material slowly increased. When the content of PPTA reached the peak at 7%, the hardness of the composite was 61.2, which was similar to the hardness of unmodified PTFE. When 3% nano Al_2O_3 particles and PPTA were compounded and modified into PTFE, the hardness of the PTFE composite material increased slightly from 62 to 64.2 degrees, an increase of 4.8%, indicating that ceramic particles could effectively increase the hardness of PTFE. By comparing the two materials, it can be seen that the hardness of the composite material increased first and then decreased. Three percent nano Al_2O_3 particles could increase the hardness of the composite material on the basis of only filling PPTA.

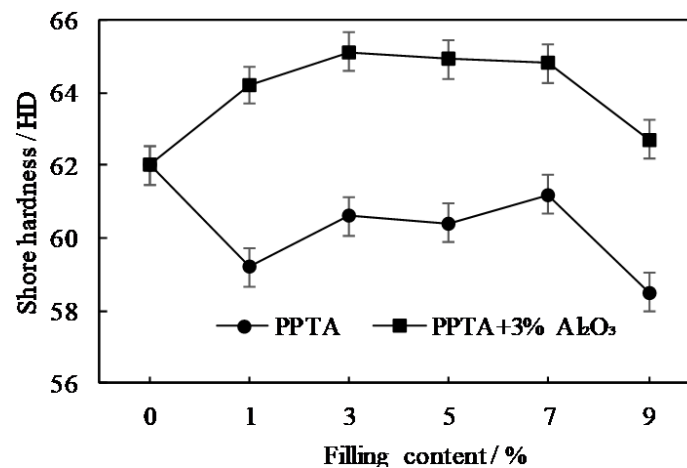


Figure 15. The hardness of PPTA and nano Al₂O₃ particles filled modified PTFE composite material.

4.2.2. Impact Performance

The impact properties of modified PTFE filled with PPTA and nano Al₂O₃ particles were tested. The impact performance of the composite material is shown in Figure 16. It can be seen from the figure that the addition of PPTA significantly reduced the impact toughness of PTFE. When the filling amount of PPTA was 5%, the impact toughness of the composite material decreased from the original 17.89 to 4.46 kJ/m², a decrease of 75%, which was due to the poor bonding force between PPTA and Al₂O₃ and the PTFE matrix. In addition, the impact performance of composite materials was mainly affected by fibers, because fibers would significantly affect the failure mode of composite materials during the impact process. The impact strength was sensitive to the notch of the sample, and all impact energy was absorbed in the notch. Therefore, the impact strength had higher requirements for the interface bonding performance of composite materials. However, the impact properties of PPTA composites decreased significantly. The impact strength after adding Al₂O₃ was similar to that of PPTA.

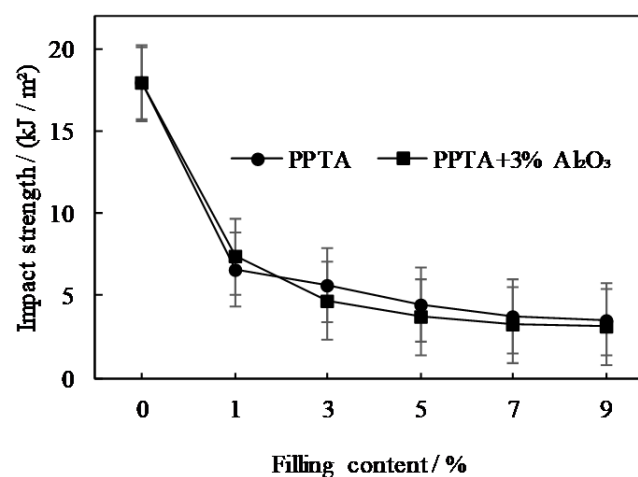


Figure 16. Impact performance of PPTA and nano Al₂O₃ particles filled modified PTFE composites.

4.2.3. Tensile Performance

Tensile properties of PPTA and nano Al₂O₃ particles filled modified PTFE were tested. The tensile strength, tensile elongation at break and elastic modulus of PPTA modified PTFE are shown in Figures 17–19.

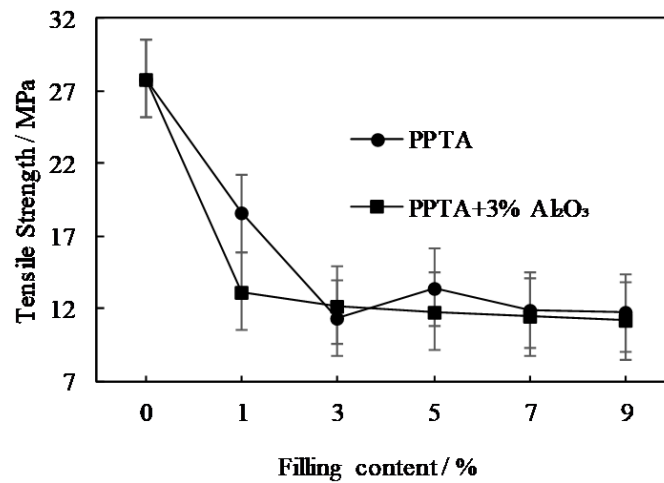


Figure 17. Tensile strength of PPTA and nano Al₂O₃ filled modified PTFE composite.

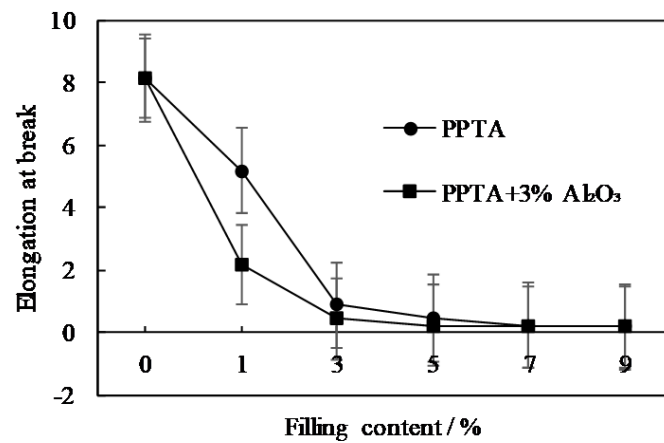


Figure 18. Tensile elongation at break of PPTA and nano Al₂O₃ filled modified PTFE composites.

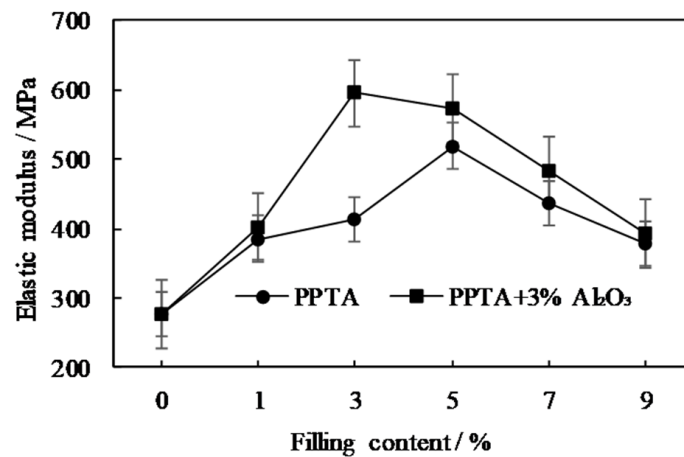


Figure 19. Elastic modulus of PPTA and nano Al₂O₃ filled modified PTFE composite.

It can be seen from Figures 17 and 18 that the tensile strength and elongation at break of PTFE were significantly reduced by adding PPTA. When the PPTA content was 1%, the tensile strength of the composite material dropped from the original 27.9 to 18.6 MPa, with a decrease rate of 33%. At this time, the tensile elongation at break decreased from the original 810–520%, which was only 64% of that of unmodified PTFE at break. When 3% nano Al₂O₃ particles and PPTA were compounded and modified into PTFE, the composite tensile strength further dropped to 13.2 MPa, which was only 50%

of the tensile strength of unmodified PTFE, while the tensile elongation at break decreased to 215%, which was only 26% of unmodified PTFE tensile elongation at break. With the increase of the PPTA content, the tensile strength of the composite material did not change significantly, while the tensile elongation at break further decreased. When the PPTA content was 9%, the tensile elongation at break of the composite material was only 16%. It can be seen from Figure 19 that PPTA and nano Al_2O_3 particles rapidly increased the elastic modulus of PTFE. When PPTA was added at 5%, the elastic modulus reached the highest point of 519 MPa, which was 1.8 times that of unmodified PTFE. With the further increase of PPTA content, the elastic modulus of the composite material gradually decreased. When 3% nano Al_2O_3 particles were compounded and modified with PPTA, the elastic modulus of the composite material was further improved on the basis of only PPTA. Among them, when the addition amount of nano Al_2O_3 particles and PPTA was 3%, the elastic modulus reached the highest point 595 MPa.

With the increase of PPTA, PPTA and PTFE in the composite material were entangled with each other, resulting in a rapid increase in the elastic modulus of the composite material. When the amount of PPTA added was 5%, the elastic modulus began to decrease gradually. This is because when the content of PPTA was high, the PTFE matrix material could not completely wrap the PPTA fibers, resulting in contact between some PPTA fibers and PPTA fibers. However, there was only an electrostatic force between PPTA and PPTA as the binding force, which led to the decrease of composite properties. It can be seen from the tensile strength that the addition of PPTA significantly reduced the tensile properties of PTFE, because the C–C bond on the PTFE surface was wrapped by F atoms, and the F atoms were relatively stable. Thus, the PPTA fiber and the PTFE matrix interface could not form a strong bonding force, only the interaction of physical meshing and electrostatic force was generated. Moreover, the bonding force was relatively weak, resulting in the gradual decline of the tensile properties of the material.

In order to further study the influence of PPTA on the properties of PTFE and the strengthening mechanism, the tensile and impact sections of the sample were observed by SEM. The SEM images of the tensile fracture surface and the impact fracture surface are shown in Figure 20. It can be seen from the figure that the PPTA fiber and PTFE matrix material were entangled with each other. The impact fracture surface presents ductile fracture, and the interface bond lacked flexibility. It can be seen from the fracture surface that the PPTA thread that was obviously drawn from the other fracture surface protrudes from the fracture surface, indicating that the bonding performance between PPTA and the PTFE matrix was poor. When impact fracture or tensile fracture occurred, there was a clear boundary layer between PPTA and PTFE. Due to the small interaction between PTFE matrix and PPTA, PPTA will pull out from PTFE and eventually lead to the fracture of the composite.

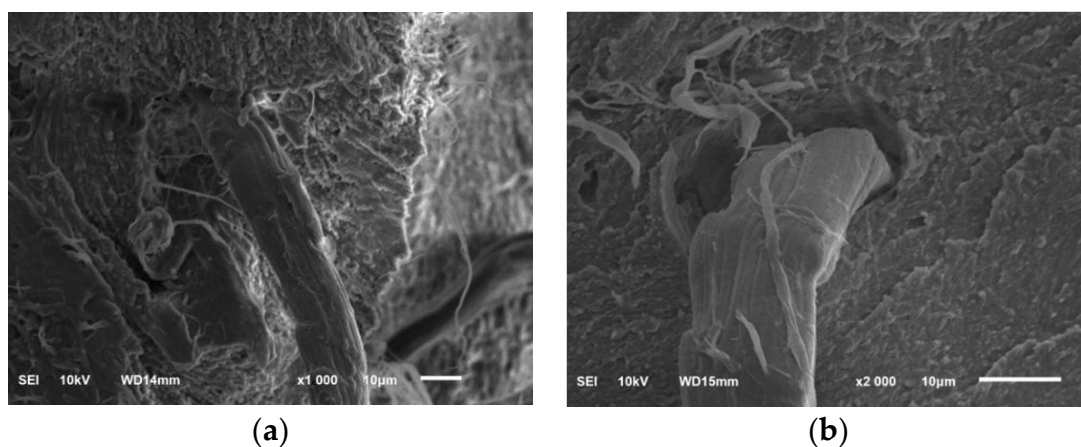


Figure 20. SEM image of cross section of PPTA modified composite material: (a) stretched section view and (b) impact section.

4.2.4. Friction and Wear Performance

In the study, the friction and wear properties of PPTA and nano Al_2O_3 filled modified PTFE were tested. The friction coefficient and wear rate of the composite material are shown in Figures 21 and 22. It can be seen from Figure 21 that the addition of PPTA and nano- Al_2O_3 particles improved the friction coefficient of the composite material. It can be seen from Figure 22 that the wear rate of the composite material was significantly improved. When the PPTA filling amount was 1%, the wear rate of the composite material dropped from the original 7.85×10^{-4} to $5.18 \times 10^{-4} \text{ mm}^3/\text{Nm}$, a decrease of 35%. It can be found that the ability of the composite material to resist plastic deformation was significantly improved, and the ploughing effect of the grinding parts on the surface of the composite material was reduced. The addition of PPTA could effectively reduce material loss and improve friction and wear performance. With the increase in the mass fraction of PPTA, the friction coefficient of the composite material increased slightly by 6–12%, mainly because the composite material formed a thicker transfer film during the adhesive wear process. With the addition of PPTA, the friction torque increased and the friction coefficient also increased. In addition, with the increase of PPTA content, the wear rate of the composite material decreased first and then rose. Among them, when the content of PPTA was 5%, the wear rate of the composite material was the lowest at $2.47 \times 10^{-4} \text{ mm}^3/\text{Nm}$, with a decrease rate of 68%.

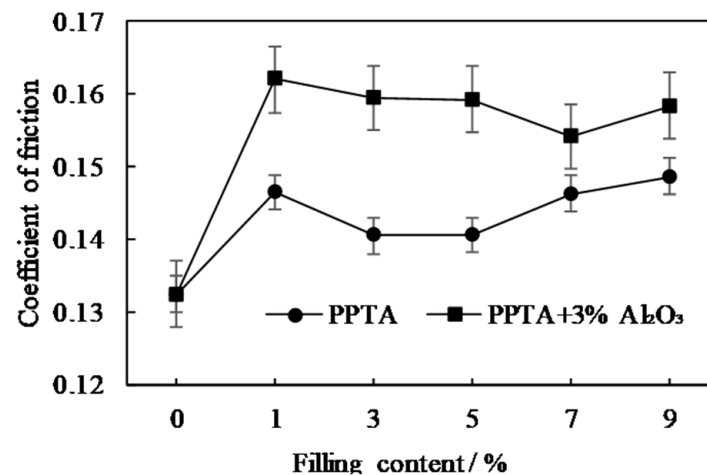


Figure 21. Wear coefficient of modified PTFE composite filled with PPTA and nano Al_2O_3 particles.

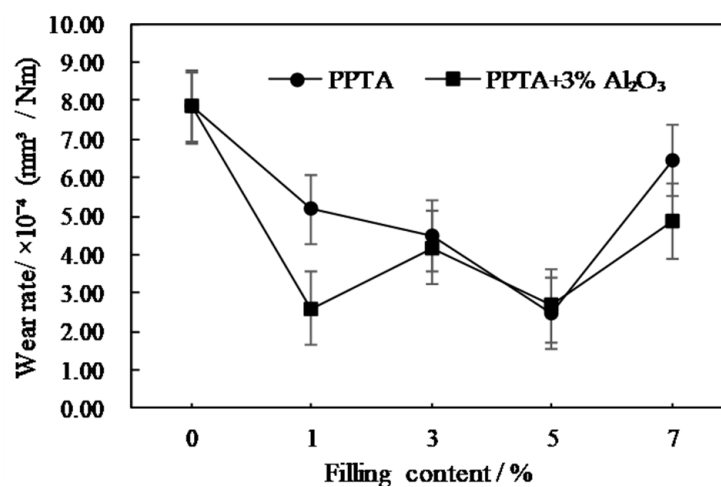


Figure 22. Wear rate of PPTA and nano Al_2O_3 particles filled modified PTFE composite.

When the content of PPTA exceeded a certain amount, the wear rate of the composite material presented an instantaneous surge. This is mainly because the composite material mainly adhered to

each other through the PTFE matrix and transferred the load to the fibers. Due to the large specific surface area of PPTA, when PPTA increases to a certain content, the PTFE matrix will not be able to bond with PPTA well. However, the interaction between PPTA is mainly through an electrostatic force, so the fibers are easy to be peeled off and pulled out, which makes the overall performance of the composite material drop sharply.

In order to further study the wear mechanism of the composites, the wear surface was tested by SEM and the surface morphology after wear was observed. The wear morphology of the composite material under dry friction conditions is shown in Figure 23.

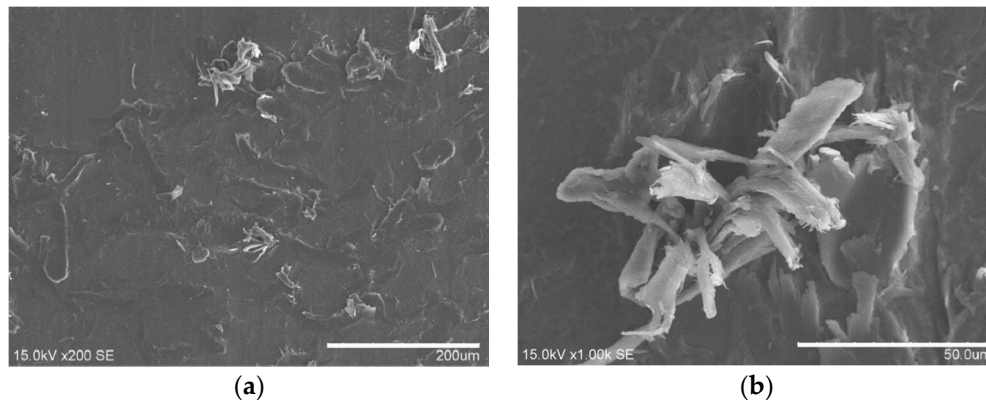


Figure 23. SEM image of the wear surface of 5% PPTA filled PTFE: (a) the magnification 200 \times ; (b) the magnification 1000 \times .

It can be seen from Figure 23 that there were obvious PPTA fibers distributed, and a little PPTA pulled out on the wear surface. The wear surface of the composite material was rough. PTFE exhibited large flakes, without obvious adhesive wear. The PPTA fiber was exposed on the wear surface of the composite material and had poor bonding performance with the matrix material. When PPTA was added into PTFE, PPTA mainly played the role of bearing and restraining the slippage of PTFE macromolecules, so as to effectively improve the wear resistance of the composite material.

5. Conclusions

- (1) Through the ultrasonic dispersion of CF and MWCNT and various processes (crushing, stirring volatilization, crushing and sieving) of PTFE materials, the effective dispersion of CF and MWCNT in the composite material and the stability of the composite material performance obtained an effective guarantee.
- (2) Through testing the hardness and impact performance of CF and MWCNT filled modified PTFE composites, it was found that various carbon materials would cause the hardness and impact toughness of PTFE composites to decrease to varying degrees. Among them, the hardness of MWCNT-filled PTFE composites decreased most obviously. When the content of MWCNT was 1%, the impact hardness of the composite material dropped from 62 to 52, with a decrease of 15.3%.
- (3) By testing the tensile properties of CF and MWCNT filled modified PTFE composites, it was found that the addition of various carbon materials would significantly reduce the tensile strength and elongation at break of PTFE, but greatly enhanced the elastic modulus. Among them, the addition of 7 μm CF reduced the tensile strength of the PTFE composite material from 27.9 MPa by about 20%, and the tensile elongation at break decreased by about 30%. The addition of MWCNT significantly reduced the tensile strength and tensile elongation at break of PTFE composites, by 60% and 87% respectively. Among them, the addition of 7 μm and 200 nm CF increased the elastic modulus of PTFE by about 70% to 471.95 MPa and 137% to 655 MPa from the original 276.8 MPa. MWCNT had a greater impact on the elastic modulus of PTFE composites.

The addition of 1% MWCNT increased the elastic modulus of PTFE from 276.8 to 1075 MPa, with an increase of 388%.

- (4) Through the friction and wear test of 200 nm and 7 μm CF and MWCNT filled PTFE composite materials, it was found that when 7 μm CF was used as the modified filler and the mass fraction was 1.5%, the composite wear rate decreased from 7.8463×10^{-4} to $2.5124 \times 10^{-4} \text{ mm}^3/\text{Nm}$, with a decrease rate of 58%. Then the wear rate of the composite material increased slightly. When 200 nm CF was used as the modified filler and the mass fraction was 1%, the wear rate of the composite material decreased from 7.8463×10^{-4} to $3.9038 \times 10^{-4} \text{ mm}^3/\text{Nm}$, with a decrease rate of 50.3%. Then the wear rate gradually increased. When MWCNT was used as a modified filling and the mass fraction was only 0.5%, the wear rate of the composite material decreased from 7.8463×10^{-4} to $2.5897 \times 10^{-4} \text{ mm}^3/\text{Nm}$, with a decrease rate of 57%.
- (5) Through the hardness and impact toughness test of PPTA and nano Al_2O_3 particle composite modified PTFE, it was found that the increase of PPTA and nano Al_2O_3 particles reduced the hardness and impact toughness of PTFE. When the PPTA content was 1%, the shore hardness of the composite material dropped from 62 to 59.2, with a decrease rate of 4.5%. When the content of PPTA was 5%, the impact hardness of the composite material dropped from the original 17.89 to 4.46 kJ/m^2 , with a decrease of 75%.
- (6) Through the tensile performance test of PPTA and nano Al_2O_3 particles composite modified PTFE, it was found that the increase of PPTA and nano Al_2O_3 particles could effectively increase the elastic modulus of PTFE. Among them, PPTA composite modification had a more obvious increase in the elastic modulus of PTFE. As the content of PPTA increased, the elastic modulus of the composite material first rose and then fell. When PPTA was added at 5%, the elastic modulus reached the highest value of 519 MPa. With the increase of filler content, the tensile strength and tensile elongation of PTFE composite material modified by PPTA fiber and nano- Al_2O_3 decreased.
- (7) By testing the friction and wear properties of PPTA and nano- Al_2O_3 composite modified PTFE, it was found that the addition of PPTA and nano- Al_2O_3 particles could significantly increase the wear rate of the composite. When the PPTA filling amount was 1%, the wear rate of the composite material dropped from the original 7.85×10^{-4} to $5.18 \times 10^{-4} \text{ mm}^3/\text{Nm}$, with a decrease of 35%.

Author Contributions: Conceptualization, F.Z. and Y.Z.; validation, J.Z. and Y.J.; formal analysis, F.Z. and X.W.; resources, F.Z.; writing—original draft, J.Z.; writing—review and editing, F.Z.; visualization, J.Z.; supervision, F.Z. All authors have read and agreed to the published version of the manuscript.

Funding: This research was supported by A Priority Academic Program Development of Jiangsu Higher Education Institutions (PAPD); Engineering Research Center for Harmless Treatment and Resource Utilization of Aluminum Ash and Slag Solid Waste in Jiangsu Province; Nantong Applied Research Project, grant number JC2018115 and JC2019129; Ministry of Education's Cooperative Education Project, grant number 201901189019.

Acknowledgments: Sincere thanks go to the anonymous reviewers for their valuable comments and good suggestions to improve this article.

Conflicts of Interest: The authors declare no conflict of interest.

References

1. Sato, Y.; Murahara, M. Protein adsorption on PTFE surface modified by ArF excimer laser treatment. *J. Adhes. Sci. Technol.* **2004**, *18*, 1545–1555. [[CrossRef](#)]
2. Liu, Y.; Xu, N.; Wang, Y.; Yao, Y.; Xiao, H.; Jia, J.; Lv, H.; Zhang, D. Preparation and tribological properties of hybrid PTFE/Kevlar fabric self-lubricating composites. *Surf. Coat. Technol.* **2019**, *361*, 196–205. [[CrossRef](#)]
3. Ashrafi, F.; Lavasani, M.R.B. Improvement of the mechanical and thermal properties of polyester nonwoven fabrics by PTFE coating. *Turk. J. Chem.* **2019**, *43*, 760–765. [[CrossRef](#)]
4. Villalobos, G.J.; Dow, N.; Milne, N.; Zhang, J.; Naidoo, L.; Gray, S.; Duke, M. Membrane distillation trial on textile wastewater containing surfactants using hydrophobic and hydrophilic-coated polytetrafluoroethylene (PTFE) membranes. *Membranes* **2018**, *8*, 31. [[CrossRef](#)]

5. He, G.; Zeng, F.; Lei, K.; Xia, S.; Deng, L.; Zhang, C.; Liu, D. Handle operation lug type ptfе lined butterfly valve (TD71X). *Eur. J. Hosp. Pharm.* **2017**, *24*, 162. [[CrossRef](#)]
6. Haque, R.I.; Briand, D. Triboelectric freestanding flapping film generator for energy harvesting from gas flow in pipes. *Smart Mater. Struct.* **2019**, *28*, 085002. [[CrossRef](#)]
7. Feng, S.; Zhong, Z.; Wang, Y.; Xing, W.; Drioli, E. Progress and perspectives in PTFE membrane: Preparation, modification, and applications. *J. Membr. Sci.* **2018**, *549*, 332–349. [[CrossRef](#)]
8. Yanhai, C.; Lu, R.; Xianliang, M.; Jinyong, Y.; Xianhua, T. The effect of PTFE addition on mechanical and anti-corrosion properties of coating of heat exchangers. *Mater. Res. Express* **2019**, *6*, 085207. [[CrossRef](#)]
9. Wang, J.; Wu, D.; Li, X.; Zhang, M.; Zhou, W. Poly (vinylidene fluoride) reinforced by carbon fibers: Structural parameters of fibers and fiber-polymer adhesion. *Appl. Surf. Sci.* **2012**, *258*, 9570–9578. [[CrossRef](#)]
10. Luo, F.; Tang, B.; Fang, Z.; Yuan, Y.; Li, H.; Zhang, S. Polytetrafluoroethylene based, F8261 modified realization of $\text{Li}_2\text{SnMg}_{0.5}\text{O}_{3.5}$ filled composites. *Appl. Surf. Sci.* **2020**, *503*, 144088. [[CrossRef](#)]
11. Shi, Y.; Feng, X.; Wang, H.; Lu, X. The effect of surface modification on the friction and wear behavior of carbon nanofiber-filled PTFE composites. *Wear* **2008**, *264*, 934–939. [[CrossRef](#)]
12. Gürgen, S.; Çelik, O.N.; Kuşhan, M.C. Tribological behavior of UHMWPE matrix composites reinforced with PTFE particles and aramid fibers. *Compos. B Eng.* **2019**, *173*, 106949. [[CrossRef](#)]
13. Yao, S.S.; Jin, F.L.; Rhee, K.Y.; Hui, D.; Park, S.J. Recent advances in carbon-fiber-reinforced thermoplastic composites: A review. *Compos. B Eng.* **2018**, *142*, 241–250. [[CrossRef](#)]
14. Ni, H.; Zhang, J.; Lv, S.; Wang, X.; Pei, Y.; Li, F. Coating process parameters and structural properties of the tubular electrodes of fuel cells based on a self-made coating device. *Coatings* **2020**, *10*, 830. [[CrossRef](#)]
15. Subramanian, R.; Shanmugam, K.; Marappan, S. Fabrication of robust superhydrophobic coatings using PTFE-MWCNT nanocomposite: Supercritical fluid processing. *Surf. Interface Anal.* **2018**, *50*, 464–470. [[CrossRef](#)]
16. Xu, F.; Fan, W.; Zhang, Y.; Gao, Y.; Jia, Z.; Qiu, Y.; Hui, D. Modification of tensile, wear and interfacial properties of Kevlar fibers under cryogenic treatment. *Compos. B Eng.* **2017**, *116*, 398–405. [[CrossRef](#)]
17. Liu, K.; Yang, W.; Peng, T.; Wang, F. Progress in Surface Modification of Aramid Fiber (II)—Chemical Modification. *Synth. Fiber China* **2011**, *40*, 26–31. (In Chinese) [[CrossRef](#)]
18. Gonzalez-Canche, N.G.; Flores-Johnson, E.A.; Carrillo, J.G. Mechanical characterization of fiber metal laminate based on aramid fiber reinforced polypropylene. *Compos. Struct.* **2017**, *172*, 259–266. [[CrossRef](#)]
19. Ni, H.; Zhang, J.; Lv, S.; Gu, T.; Wang, X. Performance optimization of original aluminum ash coating. *Coatings* **2020**, *10*, 831. [[CrossRef](#)]
20. Ni, H.; Zhang, J.; Lv, S.; Wang, X.; Zhu, Y.; Gu, T. Preparation and performance optimization of original aluminum ash coating based on plasma spraying. *Coatings* **2019**, *9*, 770. [[CrossRef](#)]
21. Shuashuai, L.; Jiaqiao, Z.; Hongjun, N.; Xingxing, W.; Yu, Z.; Tao, G. Study on preparation of aluminum ash coating based on plasma spray. *Appl. Sci.* **2019**, *9*, 4980.
22. Vasilev, A.P.; Okhlopkova, A.A.; Struchkova, T.S. Investigation of the influence of complex fillers on the properties and structure of polytetrafluoroethylene. *J. Frict. Wear* **2018**, *39*, 427–432. [[CrossRef](#)]
23. Ohlopkova, A.A.; Struchkova, T.S.; Vasilev, A.P. Studying the properties and structure of polytetrafluoroethylene filled with Belum modified carbon fibers. *J. Frict. Wear* **2016**, *37*, 529–534. [[CrossRef](#)]
24. Bajpai, A.; Saxena, P.; Kunze, K. Tribo-mechanical characterization of carbon fiber-reinforced cyanate ester resins modified with fillers. *Polymers* **2020**, *12*, 1725. [[CrossRef](#)]
25. Saxena, P.; Schinzel, M.; Andrich, M. Development of a novel test-setup for identifying the frictional characteristics of carbon fibre reinforced polymer composites at high surface pressure. *IOP Conf. Ser. Mater. Sci. Eng.* **2016**, *149*, 012124. [[CrossRef](#)]
26. Luo, F.; Tang, B.; Yuan, Y. Microstructure and microwave dielectric properties of $\text{Na}_{1/2}\text{Sm}_{1/2}\text{TiO}_3$ filled PTFE, an environmental friendly composites. *Appl. Surf. Sci.* **2018**, *436*, 900–906. [[CrossRef](#)]
27. Yuan, Y.; Li, Z.; Cao, L. Modification of Si_3N_4 ceramic powders and fabrication of Si_3N_4 /PTFE composite substrate with high thermal conductivity. *Ceram. Int.* **2019**, *45*, 16569–16576. [[CrossRef](#)]
28. Van Rooyen, L.J.; Bissett, H.; Khoathane, M.C. Gas barrier properties of oxyfluorinated graphene filled polytetrafluoroethylene nanocomposites. *Carbon* **2016**, *109*, 30–39. [[CrossRef](#)]
29. GB/T 2411-2008. *Plastics and Ebonite-Determination of Indentation Hardness by Means of a Durometer (Shore Hardness)*; China National Standardization Management Committee: Beijing, China, 2008. (In Chinese)
30. GB/T1040-2006. *Determination of Tensile Properties of Plastics*; China National Standardization Management Committee: Beijing, China, 2006. (In Chinese)

31. GB/T1043-2008. *Determination of Impact Properties of Plastic Simply Supported Beams*; China National Standardization Management Committee: Beijing, China, 2008. (In Chinese)
32. Jiang, B.; Zhu, A.; Zhang, C.; Li, Y. Interface enhancement between polytetrafluoroethylene and glass fibers modified with a titanate coupler. *J. Appl. Polym. Sci.* **2017**, *134*. [[CrossRef](#)]
33. Lv, S.; Zhang, J.; Ni, H.; Wang, X.; Zhu, Y.; Chen, L. Study on the coupling relationship of low temperature fluidity and oxidation stability of biodiesel. *Appl. Sci.* **2020**, *10*, 1757. [[CrossRef](#)]
34. Paul, R.; Bhowmik, S. Tribological Behavior of micro coir filler reinforced polymer composite under dry, wet, and heated contact condition. *J. Nat. Fibers* **2020**, 1–16. [[CrossRef](#)]
35. Zhang, J.; Kang, X.; Ni, H.; Ren, F. Surface defect detection of steel strips based on classification priority YOLOv3-dense network. *Ironmak. Steelmak.* **2020**, 1–12. [[CrossRef](#)]
36. Ni, H.; Wang, K.; Lv, S.; Wang, X.; Zhuo, L.; Zhang, J. Effects of concentration variations on the performance and microbial community in microbial fuel cell using swine wastewater. *Energies* **2020**, *13*, 2231. [[CrossRef](#)]
37. Ni, H.; Wang, K.; Lv, S.; Wang, X.; Zhang, J.; Zhuo, L.; Li, F. Effects of modified anodes on the performance and microbial community of microbial fuel cells using swine wastewater. *Energies* **2020**, *13*, 3980. [[CrossRef](#)]
38. Wang, L.; Duan, Y.; Zhang, Y.; Huang, R.; Dong, Y.; Huang, C.; Zhou, B. Surface modification of poly-(p-phenylene terephthalamide) pulp with a silane containing isocyanate group for silicone composites reinforcement. *Wuhan Univ. J. Nat. Sci.* **2016**, *21*, 505–511. [[CrossRef](#)]

Publisher's Note: MDPI stays neutral with regard to jurisdictional claims in published maps and institutional affiliations.



© 2020 by the authors. Licensee MDPI, Basel, Switzerland. This article is an open access article distributed under the terms and conditions of the Creative Commons Attribution (CC BY) license (<http://creativecommons.org/licenses/by/4.0/>).